1 May 1998

ELSEVIER

Chemical Physics Letters 287 (1998) 403–411

CHEMICAL PHYSICS LETTERS

The cavity ring-down absorption spectrum of the $S_0 \rightarrow T_1$ and $S_0 \rightarrow S_1$ transition of jet-cooled 4-H-1-benzopyrane-4-thione

A.A. Ruth [a,*], T. Fernholz [a], R.P. Brint [b], M.W.D. Mansfield [a]

[a] *Department of Physics, National University of Ireland, University College, Cork, Ireland*
[b] *Department of Chemistry, National University of Ireland, University College, Cork, Ireland*

Received 26 January 1998; in final form 12 February 1998

Abstract

The very sensitive cavity ring-down method has been applied to the measurement of the absorption of 4-H-1-benzopyrane-4-thione (BPT) in a supersonic jet in the wavelength region of the $S_0 \rightarrow T_1$ and $S_0 \rightarrow S_1$ transition between 15800 and 16650 cm^{-1}. The absorption energies of vibronic states corroborate previous assignments in the multi-photon excitation and $S_0 \rightarrow T_1$ phosphorescence excitation spectra of jet-cooled BPT. The symmetry forbidden 0,0 transition, $S_{0,0} \rightarrow S_{1,0}$ at 16522 cm^{-1}, was found to be 7.5 times weaker than the absorption transition to the triplet origin, $S_{0,0} \rightarrow T_{1z,0}$.

1. Introduction

In a recent publication [1] the $S_0 \rightarrow T_1$ phosphorescence excitation spectrum of jet-cooled 4-H-1-benzopyrane-4-thione (BPT) was reported. In the excitation region up to ≈ 1700 cm^{-1} above the T_1 origin at 15828 cm^{-1} *no* spectral features were observed that could be attributed to $S_{0,0} \rightarrow S_{1,v}$ transitions for the following photophysical reasons: The quantum yield ϕ_{S_1} of the $S_1 \rightarrow S_0$ fluorescence is extremely low for large thiones in general and for BPT a prompt fluorescence has never been observed upon excitation to S_1 [2]. Since non-radiative decay channels dominate the relaxation from S_1, the measurement of an $S_0 \rightarrow S_1$ fluorescence excitation spectrum is not feasible in BPT. Furthermore, although the phosphorescence quantum yield ϕ_{T_1} is high for BPT (≈ 0.13 in a perfluoroalkane [3]), a $T_1 \rightarrow S_0$ emission cannot be observed after $S_0 \rightarrow S_1$ excitation because the triplet manifold is effectively not populated by intersystem crossing $S_1 \rightsquigarrow T_1$ *in the isolated molecule*. The small energy gap $\Delta E(S_1,T_1)$ of ~ 600 cm^{-1} causes the singlet and triplet manifold to be virtually decoupled at low excess energies above $T_{1,0}$ [1,4].

As demonstrated in Ref. [5], however, the S_1 manifold of jet-cooled BPT can be investigated through resonance-enhanced multi-photon excitation $S_{0,0} \overset{h\nu}{\rightarrow} S_{1,v} \overset{n \cdot h\nu}{\rightarrow} \Psi_{S,T}$ by detecting the fluorescence from higher vibronic S_2 states $S_{2,v''} \rightarrow S_{0,v'}$ and/or the emission from a photofragment. In Ref. [5] it was not possible to compare the absolute absorption of $T_{1z,0}$ with that of $S_{0,0}$, owing to the multi-photon nature of the excitation process. The objective of this publication is to corroborate the data in Refs. [1,5] by *direct absorption* measurements. Considering the

* Corresponding author.

0009-2614/98/$19.00
PII: S0009-2614(98)00176-6

low molecular density in a seeded supersonic jet and the weakness of the $S_0 \rightarrow S_1$ and $S_0 \rightarrow T_1$ absorption transitions in jet-cooled BPT (oscillator strengths $f \sim 10^{-4}$), conventional absorption techniques appear to be insufficient. Therefore the extremely sensitive cavity ring-down (CRD) method [6] was applied. In CRD absorption spectroscopy a laser pulse is stored in a stable high-finesse optical cavity, formed by two highly reflecting mirrors, which contains the gaseous sample. Due to the losses of the cavity the intensity of the light transmitted through one of the mirrors decays exponentially with the ring-down time τ_{crd}. The losses of the cavity are only dependent on the reflectivity $R(\tilde{\nu})$ of the mirrors, the length l of the cavity (diffraction losses) and the wavelength dependent absorption of the sample molecules. For small losses (i.e. high mirror reflectivity, small absorption cross-sections) the decay rate $\tau_{crd}^{-1}(\tilde{\nu})$ is directly proportional to the total losses; thus, the absorbance per pass of the sample, α, can be easily obtained by the known quantities τ_{crd}^{-1}, R and l (see Eq. (A.1) in the Appendix).

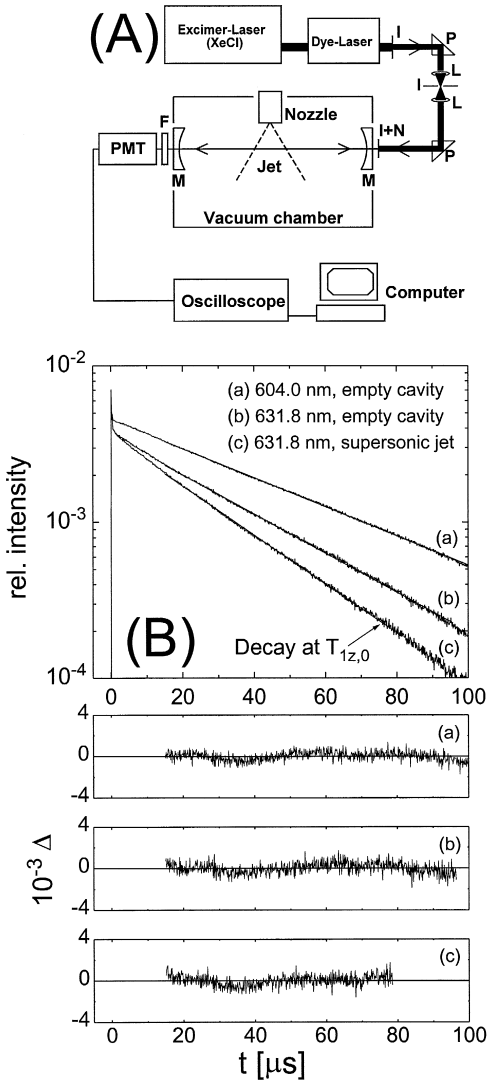

Fig. 1. (A) Experimental apparatus schematically. The light pulse from the excimer-pumped dye laser was spatially filtered in order to reduce ASE; it was then coupled into the high-finesse ring-down cavity, formed by two highly reflecting mirrors ($R > 99.99\%$) in a high vacuum chamber. The optical axis was intercepting a pulsed molecular jet. M: Mirrors, PMT: Photomultiplier Tube, L: Lenses, P: Prisms, I: Iris, N: Neutral Density Filter, F: Filter (optional). (B) Cavity ring-down decays and linear regression data at 604 and 631.8 nm for the empty cavity (trace (a): 21416 s^{-1}, trace (b): 28810 s^{-1}) as well as for jet-cooled BPT (trace (c): 36070 s^{-1}). The residuals (relative deviations) are shown in the lower part of the figure.

From the near UV to the near IR methods of cavity ring-down spectroscopy have been shown to be sufficiently sensitive to detect extremely weak absorption transitions in a variety of molecular compounds in the gas phase or in molecular jets [7–13]. However, CRD spectroscopy has not yet been applied to singlet–triplet transitions of large aromatic compounds in seeded molecular jets.

2. Experiment

The experimental set-up for CRD measurements of the $S_0 \rightarrow T_1$ absorption of jet-cooled BPT is shown schematically in Fig. 1(A).

2.1. The cavity ring-down system

Laser light from an excimer-pumped pulsed dye laser (Lumonics EX-700, XeCl; Lumonics HD-300; rhodamine B) with a pulse duration of $\tau_p \approx 15$ ns and a spectral resolution of $\lesssim 0.3$ cm^{-1} is coupled into an optically stable resonator, formed by two equal spherical mirrors. The dielectric coating on the concave side of each mirror has a specified reflectivity of $R \gtrsim 99.99\%$ between 580 and 630 nm, the flat side is anti-reflection coated [1]. The mirrors (diameter

[1] The mirrors were purchased from Research Electro Optics, Boulder, CO, USA.

25.4 mm, radius of curvature 2 m) with a separation of $l \approx 770.5$ mm are mounted on adjustable bellows at the end of a vacuum chamber. The separation corresponds to a round-trip time of $\tau_r \sim 5.1\,\text{ns} < \tau_p$. The decay of the light intensity in the cavity was monitored with a red-sensitive photomultiplier (Philips XP2254/B), whose output signal at a medium photocathode voltage was measured directly with a digital oscilloscope (LeCroy 9410), which was interfaced to a computer. For scans over wide wavelength ranges and particularly at the limits of the laser-dye the high voltage of the PMT was adjusted accordingly so that the amplitude of the signal does not change considerably. For an empty cavity the longest ring-down time of $\tau_{crd} = 68\,\mu\text{s}$ was found at ~ 610 nm, which corresponds to $R = 0.99996$. Decay curves were typically sampled over 100 shots. Three typical decay curves are shown in Fig. 1(B). The determination of the ring-down time from the exponential decay with a nonlinear least-square method (Marquardt Algorithm), using an exponential fit function of the form $a_1 + a_2 \exp(-a_3 t)$, proved to be rather noisy owing to the strong correlation between the fit parameters a_1 (offset), a_2 (amplitude) and a_3 (decay rate constant). The treatment of the offset, due to the dark counts of the PMT and 'electrical noise', is crucial in the determination of τ_{crd}. The following linear regression procedure yielded a considerably better signal-to-noise ratio than the fit: After subtraction of a small offset, determined from the weak background signal before the laser is fired ($t = 0$), the datapoints were low-pass filtered by subsequent integration over 25 datapoints [2]. A linear regression of the logarithm of the filtered data yielded the ring-down time in a reliable and quick way. For the regression only the central part of the decay curve was taken into account, since the time dependence of the intensity in the cavity was easily affected by (i) a saturation effect of the PMT cathode at medium to high laser pulse energies and (ii) by the small amount of amplified spontaneous emission (ASE) which is present in the laser light. Both effects are demonstrated in Fig. 1(B). The short spike right after laser excitation is mostly due to transverse modes of very high order, which are efficiently damped in the resonator. This can lead to a transient saturation of the photocathode in a short time interval which manifests itself in a deviation from the monoexponential time dependence in the very beginning of the decay. The effect of ASE on the decay is perceivable in the comparison of the measurement at 604 nm (center of the wavelength range of rhodamine B) with measurements at 631.8 nm (end of the wavelength range of rhodamine B), where the amount of ASE in the laser light is increased. At 631.8 nm the total decay appears slightly 'less' monoexponential owing to ASE containing frequencies for which the mirror reflectivity is significantly lower. (In the case shown, ASE decays faster than the laser light.) Hence, in a typical measurement approximately the first 15% of the total decay curve was omitted in the regression and datapoints with a value lower than 10% of the first regression point were left out as well. Low-pass filtering the data does not change the ring-down time, it reduces the noise level of the curve, so that the 10% limit is reached at later times. The time span covered by the regression for each of the measurements in Fig. 1(B) can be seen by means of the residuals in the lower part of the figure.

The shot-to-shot noise of the ring-down times was lower than 6% over the entire wavelength range used for the measurements, and overall diffraction losses were negligible (Fresnel number $N_F > 300$ [14]).

2.2. Preconditions for measuring singlet–triplet transitions in CRD spectroscopy

In the recent literature on CRD spectroscopy the response of a ring-down cavity to various types of excitation pulses was investigated with respect to the spectral resolution limit of the CRD technique [11,15–18]. In this context the multi-mode structure of ''short'' cavities [15] was discussed, particularly for the case of species with a long natural lifetime inside the cavity. Since a metastable triplet state with a lifetime $\tau_{T_{1z,0}}(\text{BPT}) \approx 10.5\,\mu\text{s}$ is the subject of this

[2] Instead of subtracting the mean background signal, the offset was alternatively taken into account by varying it in a second order polynomial regression such that the quadratic term approaches zero. This method yielded equally good results.

investigation, we briefly discuss the applicability of the CRD experiment to singlet–triplet transitions along the lines of the above literature.

Assuming the laser light to be mode matched to the TEM_{00} mode of the ring-down cavity, the free spectral range of our cavity would be $c/2L = 190$ MHz with an approximate width of the longitudinal modes of only $c(1-R^2)/(2\pi LR) \approx 5$ kHz (R was taken to be 0.99996, see above). Considering these values, the rotational lines of the first excited triplet state of BPT with a homogeneous halfwidth of $\Delta\nu_{hom} \approx 15$ kHz would basically not overlap with the mode structure inside the cavity and absorption lines would be missed. This assumption, however, is far from representing the real situation in our experiment, as shown by the following arguments: (a) The mode structure of the dye laser was poorly matched to the ring-down cavity, even for a perfect alignment of the laser resonator. (b) The geometry of the optically stable ring-down cavity was between the confocal and planar type of resonator ($g_{1,2} = 0.61$). By detuning the resonator away from a confocal mirror separation, exact transverse mode matching is impossible as demonstrated by Meijer et al. [11] and the superposition of longitudinal and transverse cavity modes essentially forms a continuum. (c) The ring-down cavity was not stabilized with regard to alterations of the cavity length such as mechanical vibrations or expansion of the vacuum chamber due to small temperature variations. The tiny fluctuations of the cavity length could directly be demonstrated by rapidly changing transverse mode patterns that were observable when a cw–Helium–Neon laser was passed through the resonator. Effects caused by a fluctuating length of the ring-down cavity are compensated by averaging over 100 laser shots or more. (d) Since the molecular jet was not skimmed, a maximum Doppler broadening of up to ≈ 1.5 GHz (~ 0.05 cm^{-1}) can be expected, which would overlap with roughly 8 mode-matched longitudinal modes of the resonator.

Points (a) to (d) guarantee the observability of the singlet–triplet transition of BPT at low resolution, i.e. resolution of the rotational envelope of vibronic states of the jet-cooled compound (see Section 3). In a stabilized and mode matched cavity rotational envelopes could in principle be resolved according to a method suggested by Lehmann and Romanini [16].

2.3. The jet apparatus

Synthesis and purification of 4-H-1-benzopyrane-4-thione is described in Ref. [19] and references therein. BPT was seeded into ≈ 950 mbar helium at a temperature of ≈ 98°C and expanded into vacuum through a circular pulsed nozzle with a diameter of $D = 1.2$ mm (Iota One nozzle driver, General Valve Corporation). The position of the nozzle in the ring-down cavity was adjusted perpendicular to the optical axis of the resonator so that the signal from the $S_0 \rightarrow T_1$ absorption of BPT was maximal. The supersonic jet was intercepted ~ 4.8 mm downstream from the nozzle. At a jet-pulse repetition rate of 6 Hz and a jet-pulse duration of 800 μs the total backing pressure in the vacuum chamber did not exceed 2×10^{-4} mbar, which was well within the capacity of the diffusion pump. The vacuum system was equipped with a liquid nitrogen trap, which was essential in order to avoid any type of contamination with oil vapours and other sorts of aerosols.

3. $S_0 \rightarrow T_1$ cavity ring-down absorption spectrum of BPT in a supersonic jet

The cavity-ring down absorption spectrum of BPT in a helium expansion was measured in the spectral region between 15800 and 16650 cm^{-1}. For each datapoint the cavity ring-down time was measured twice, with and without the supersonic jet passing through the resonator. The reference curve of the empty cavity was interpolated by a 4th-order polynomial and then subtracted from the actual ring-down spectrum of BPT. In this way the wavelength dependence of the mirror reflectivity was eliminated. The resulting difference spectrum is shown in Fig. 2(A). The remaining background in the spectrum derives from losses due to scattering with the carrier gas helium [3]. The evaluation of absolute extinction coefficients was only possible within substantial error limits and is therefore discussed in the Appendix.

[3] Using argon as carrier gas increases the background by ≈ 25–30%.

3.1. Comparison with the $S_0 \rightarrow T_1$ phosphorescence and multi-photon excitation spectrum

The $S_0 \rightarrow T_1$ cavity ring-down absorption (CRDA) spectrum matches the $S_0 \rightarrow T_1$ phosphorescence excitation (PE) spectrum from Ref. [1] very well. The 0,0 transition and most $S_0 \rightarrow T_{1z,v}$ transitions could be reproduced as shown in Fig. 2(B) and Table 1. The signal-to-noise ratio in the origin of the CRDA spectrum is $\approx 7{:}1$. Consequently, the very weak lines which were observed in the PE spectrum are still in the noise of the CRDA spectrum; therefore, they were not assigned. Since the PE spectrum is rate-corrected and corrected for constant excitation photon fluence, the relative intensities of vibronic transitions, normalized to $T_{1z,0}$, can be compared with the relative absorbances in the CRDA spectrum which are also normalised to the triplet origin (see Table 1). Throughout the wavelength region shown the relative absorbances in the CRDA spectrum are greater than the relative intensities in the PE spectrum. Therefore, the quantum yields of the phosphorescence from vibronic triplet states $T_{1z,v}$ are lower than for the origin $T_{1z,0}$ as may be expected and demonstrated in Fig. 3.

Although $S_0 \rightarrow S_1$ excitation occurs in the isolated molecule, the 0,0 transition to the first excited singlet state S_1 is not present in the PE spectrum mainly due to the lack of $S_1 \rightsquigarrow T_1$ ISC which prohibits the observation of subsequent $T_1 \rightarrow S_0$ phosphorescence. However, in the CRDA spectrum the $S_{0,0} \rightarrow S_{1,0}$ was observed at 16522 cm^{-1}. This corroborates the result from Ref. [5], where $S_{1,0}$ was found at 16520 in the multi-photon excitation (MPE) spectrum of BPT. The MPE spectrum, taken from Ref. [5], is shown in Fig. 2(C). The fact that the $S_{1,0}$ appears to be much stronger in the MPE spectrum than in the CRDA spectrum is by no means contradictory for the following reasons: (i) In the MPE spectrum the total emission was detected after 2-, 3-, and 4-photon absorption of a smoothly focused excitation beam. Thus, the MPE spectrum was not corrected for the fluence of the excitation light and the relative intensities of lines in Fig. 2(C) are therefore wavelength dependent. A strong $S_{1,0}$ can derive from a higher efficiency of the laser-dye in that particular wavelength region. (ii) At low to medium excitation energies most of the emission detected in the MPE spectrum is due to $S_2 \rightarrow S_0$ fluorescence (see Fig. 5 in Ref. [5]). It is likely that populating S_2 by a transient singlet absorption $S_{0,0} \rightarrow S_{1,0} \rightarrow S_{2,v}$ is more efficient than an excitation via the triplet manifold $S_{0,0} \rightarrow T_{1z,0} \rightarrow T_{n,v''} \rightsquigarrow S_{2,v'}$, owing to the inverted intersystem crossing process from the triplet to the singlet manifold at high vibronic energies. A considerable difference in the efficiency of these two

Table 1
Comparison of the lowest vibronic $S_{0,0} \rightarrow T_{1z,v}$ and $S_{0,0} \rightarrow S_{1,v}$ transitions found in the cavity ring-down absorption, phosphorescence excitation and multi-photon excitation spectrum. Wavenumbers are vacuum corrected and accurate within $\pm 2.5\,cm^{-1}$. After normalization to the 0,0 transition the relative absorbances in the CRDA spectrum can be compared with the relative intensities of lines in the phosphorescence excitation spectrum

Cavity ring-down [cm^{-1}]	Normalized absorbance	Phosphorescence excitation [cm^{-1}]	Normalized intensity	Multi-photon excitation [cm^{-1}]	Assignment
15828.2	100.0	15827.9	100.0	15828.0	$T_{1z,0}$
16004.1	15.4	16004.2	12.4	16004.9	T_{1z,v_1}
16196.7	11.2	16197.0	3.6	16197.3	T_{1z,v_2}
		16243.3	1.2	16243.1	T_{1z,v_3}
		16275.1	1.0	16273.8	T_{1z,v_4}
16337.5	8.9	16337.8	2.0	16337.6	T_{1z,v_5}
16363.2	17.7	16363.5	14.3	16364.4	T_{1z,v_6}
16427.5	9.1	16428.0	0.5	16429.5	T_{1z,v_7}
		16458.3	0.7	16459.2	T_{1z,v_8}
16484.0	14.2	16484.3	5.5	16484.2	T_{1z,v_9}
16522.3	13.3	–	–	16520.1	$S_{1,0}$
16538.2	8.4	16539.9	1.1		$T_{1z,v_1} + T_{1z,v_6}$
16613.8	9.6	16614.7	1.3	16615.7	$T_{1z,v_{10}}$
16637.1	9.9	–	–	16634.5	S_{1,v_1}

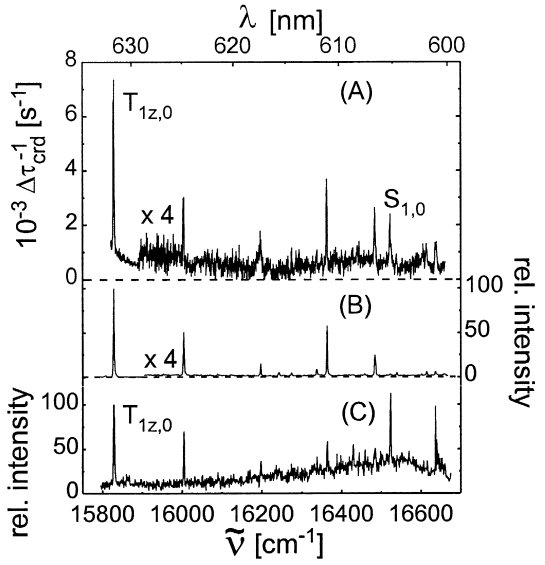

Fig. 2. (A) Upper trace: Cavity-ring down absorption spectrum of BPT in a helium expansion (≈ 1000 mbar) from 15700–16700 cm^{-1} (rhodamine B). The region above 15900 cm^{-1} has been expanded by a factor of 4 and shifted by $-380\,s^{-1}$ (B) Middle trace: Normalized and fully corrected $S_0 \rightarrow T_1$ phosphorescence excitation spectrum of BPT in a helium expansion (≈ 1000 mbar) from Ref. [1]. The region above 15900 cm^{-1} has been expanded by a factor of 4. The spectrum does not show any $S_0 \rightarrow S_1$ transitions. (C) Lower trace: Normalized multi-photon excitation spectrum of BPT in a helium expansion (≈ 1000 mbar); wavenumbers refer to single-photon energies. The emission was detected in the spectral region from ≈ 20000 to 25000 cm^{-1}, using a short time window [5]. This spectrum is neither rate-corrected nor corrected for the wavelength dependence of the fluence of the laser excitation light. All excitation wavenumbers are vacuum corrected.

excitation pathways would also explain the disproportionately strong S_1 lines in Fig. 2(C) in comparison to the ones assigned in the CRDA spectrum (Fig. 2(A)).

The absorption of $S_{1,0}$ was found to be ≈ 7.5 times weaker than the absorption of the triplet origin $T_{1z,0}$. The $S_0 \rightarrow S_1$ absorption was approximated by Nickel and Eisenberger [19] for BPT in perfluoro-1,3-dimethylcyclohexane at room temperature by subtracting the estimated $S_0 \rightarrow T_1$ spectrum [4] from the measured absorption spectrum between 450 and 660 nm. The origin band of the $S_0 \rightarrow S_1$ spectrum in solution was found to be approximately half as strong as the triplet origin $T_{1z,0}$, which is more than 3.5 times stronger than in the CRDA spectrum. In solution inhomogeneous broadening leads to the coupling of the S_1 with the T_1 manifold increasing the absorption of singlet states. Nevertheless, our result shows that approximating the $S_0 \rightarrow T_1$ absorption spectrum of BPT in solution by Förster's relation [20] is somewhat crude in the present case, although E-type delayed luminescence virtually does not contribute to the phosphorescence spectrum at room temperature.

The $T_{1z,0}$ origin is depicted in Fig. 4. Owing to the low symmetry the rotational contour of the cooled molecule shows a AB hybrid band structure for an asymmetric top with an in-plane transition moment. The rotational envelope shows a sharp origin, together with two local maxima at -1.1 cm^{-1} and 0.8 cm^{-1} from the origin, respectively. The total rotational bandwidth (fwhm) observed for the rotational envelope of the 0,0 transition of the triplet of BPT is ~ 2.8 cm^{-1} under the experimental conditions given in Section 2. This bandwidth compares to that in the phosphorescence excitation spectrum (~ 2.6 cm^{-1}), which was measured under slightly better cooling

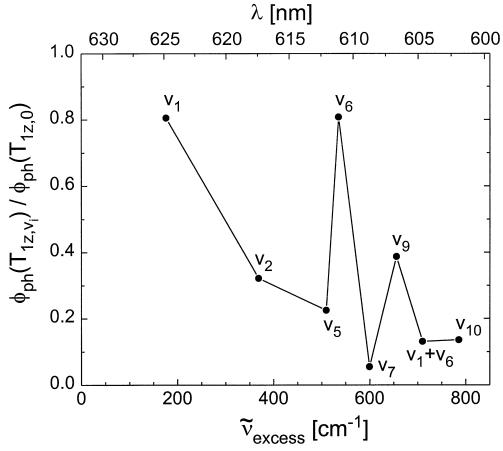

Fig. 3. Phosphorescence quantum yield Φ_{ph} of vibronic triplet states T_{1z,v_i} with respect to the origin quantum yield versus wavenumber.

[4] The $S_0 \rightarrow T_1$ absorption spectrum was estimated with Förster's [20] approximate relation between a corrected emission spectrum and the respective absorption spectrum which is based on the mirror image relation of the corresponding spectra.

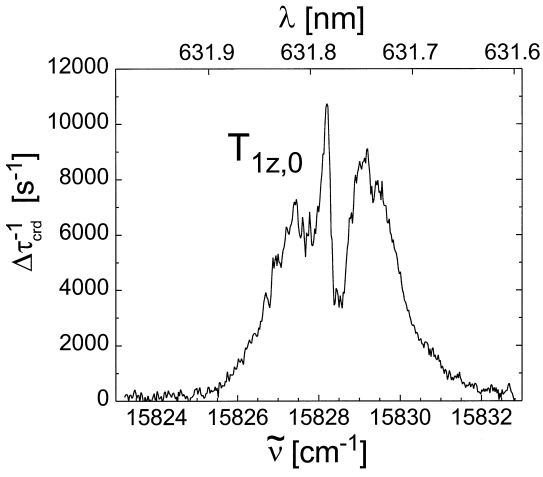

Fig. 4. Rotational envelope (AB hybrid) of the $S_{0,0} \rightarrow T_{1z,0}$ transition of jet-cooled BPT, measured with the cavity ring-down method.

conditions (1000 mbar of helium, 13 mm downstream from the nozzle of diameter 0.8 mm).

3.2. Summary

It was demonstrated that electronic singlet–triplet transitions of jet-cooled aromatic compounds can (in principle) be studied by means of CRD spectroscopy. In the particular case of 4-H-1-benzopyrane-4-thione the $S_0 \rightarrow T_1$ phosphorescence excitation spectrum was reproduced and assignments of previous publications were confirmed. The measurement of absolute absorption cross-sections proved to be difficult owing to the strong non-equilibrium situation in seeded supersonic expansions. Further investigations on 4-H-pyrane-4-thione in a static cell as well as in a supersonic jet are on the way [21].

Acknowledgements

We are very thankful to Dr. B. Nickel (MPI für Biophysikalische Chemie, Göttingen, Germany) for providing pure samples of BPT and continuously supporting our work. AAR gratefully acknowledges support by the Deutsche Forschungsgemeinschaft (Habilitationsstipendium RU 672/1–1). This work was funded by the Irish organization for science and innovation FORBAIRT (contract: SC/97/755). We would like to thank Prof. I. Mills (University of Reading, UK) for his advice regarding the rotational envelope of $T_{1z,0}$, and W.G. Doherty and E.W. Gash for their experimental assistance.

Appendix A. On the estimation of absolute extinction coefficients

This Appendix describes the procedure for the determination of *absolute* extinction coefficients in seeded beams and discusses principle difficulties encountered in our experiment.

The ring-down time τ_{crd} is related to the total absorbance α per pass by [8,11]:

$$\alpha(\tilde{\nu}) = \frac{l}{c\tau_{\mathrm{crd}}} + \ln R(\tilde{\nu}) \qquad (A.1)$$

with l being the cavity length and R the mirror reflectivity determined from the ring-down time of the evacuated cavity (assuming negligible diffraction losses). In a seeded beam the carrier gas contributes to the total losses as well, and the absorbance is given by $\alpha = \alpha_{\mathrm{He/BPT}} = \alpha_{\mathrm{He}} + \alpha_{\mathrm{BPT}}$ (α_{He} is based on the light scattering by helium). In the origin of the triplet manifold at 15828 cm^{-1} α_{BPT} was found to be $2.6 \pm 0.3 \times 10^{-5}$ per pass. The evaluation of an absolute extinction coefficient, ϵ, for the $S_0 \rightarrow T_1$ transition proved to be rather inaccurate because the number density ρ_{BPT} of BPT molecules in the jet for our expansion parameters could not be determined within acceptable error limits for several reasons: (i) The vapour pressure of BPT at 98°C in a non-thermal equilibrium situation before expansion is not known and difficult to estimate. (ii) The absorption had to be measured in the transition range of the jet-expansion at $\gtrsim 4D$, where the calculation of seed molecule densities is vague. (iii) The density of molecules in a seeded jet pulse with a duration of 800 μs is not necessarily temporally constant. We measured at maximal seed molecule density in the jet pulse, which is assumed to be independent of time over a period at least of the order of the ring-down time.

Nonetheless, an attempt was made to determine ρ_{BPT} through measuring the distribution of BPT

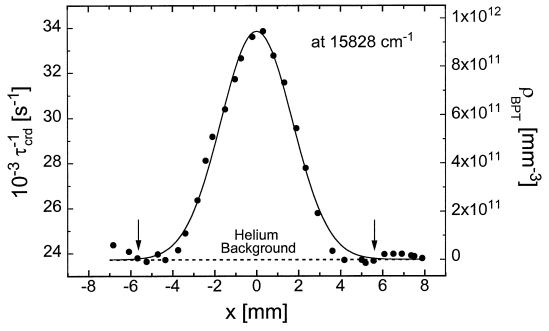

Fig. 5. Distribution of BPT molecules in a helium expansion at $z = 4.8$ mm downstream from the nozzle. The ring-down time was measured as a function of the nozzle displacement x [mm] perpendicularly across the optical axis of the resonator at 15828 cm^{-1}. The density scale (ρ_{BPT}) was estimated with Eq. (A.2). The arrows mark integration limits used in Eq. (A.3) in the Appendix.

molecules in the jet by gradually moving the nozzle perpendicularly across the optical axis of the resonator ($z = 4.8$ mm downstream from the nozzle). The excitation wavenumber was at the triplet origin at 15828 cm^{-1}. In such an experiment the *integrated distribution* of BPT molecules along a coordinate parallel to the resonator axis is probed. We found a virtually Gaussian distribution shown in Fig. 5. This particular distribution justifies the assumption of the statistical independence of the coordinates across (x) and along (y) the optical axis, because the expansion is expected to be cylindrically symmetric around the center position of the circular nozzle. In this case the beam profile represents the ''real'' spatial distribution of BPT in the jet (i.e. halfwidth and shape) at a particular distance from the nozzle. The maximum of the Gaussian distribution in Fig. 5 was scaled to the mean local density of BPT molecules in the center of the jet, $\rho_{BPT}(z = 4.8\ \text{mm}) = 9.46 \times 10^{11}\ \text{mm}^{-3}$, which was estimated with the isentropic equation

$$\rho_{BPT}(z) = P_0\left[k_B T_0\left[1 + \left(\frac{\gamma - 1}{2}\right)M^2(z)\right]^{\frac{1}{\gamma-1}}\right]^{-1}, \tag{A.2}$$

describing the adiabatic expansion. In (A.2) the Mach number $M(4.8\,\text{mm}) \approx 7.7$ was approximated using an adiabatic constant for the mixture according to the mole fractions of the two components ($\gamma = 1.648$) as well as interpolated empirical values [22]. P_0 was assumed to be ≈ 5 mbar, which is approximately 10 times smaller than the vapour pressure of BPT at $T_0 = 370$ K [21] [5]. A small value for P_0 is justified due to the non-equilibrium situation (10 Hz repetition rate) before expansion – it is the most critical assumption in this estimate.

The number of molecules per area in the laser-jet-interaction region, N_{BPT}, is in good approximation given by (for integration limits see Fig. 5):

$$N_{BPT} = \int_{-\infty}^{+\infty} \rho_{BPT}(x)\,dx \approx 3.94 \times 10^{12}\ \text{mm}^{-2}. \tag{A.3}$$

Hence, the extinction coefficient can be estimated to be $\epsilon = \alpha_{BPT}/N_{BPT} \sim 39.7\ \text{l mol}^{-1}\,\text{cm}^{-1}$ at 15828 cm^{-1}. This value is only accurate within one order of magnitude; it nonetheless suggests that the extinction coefficient in the isolated molecule is indeed greater than for BPT in solution, where the value of $\epsilon = 10.4\,\text{mol}^{-1}\,\text{cm}^{-1}\,\text{l}$ was measured [3]. However, regarding the dominance of the $T_{1z,0}$ absorption line in jet-cooled BPT in comparison to the absorption spectrum of BPT in solution, one would expect the extinction coefficient of $T_{1z,0}$ to be greater than the estimated value. The use of a slit nozzle will remove uncertainties in the expansion parameters in Eq. (A.2). The remaining error due to the unknown partial pressure of the seed molecules in the reservoir under non-equilibrium conditions is therefore the restricting factor in the determination of absolute absorption parameters.

References

[1] A.A. Ruth, F.J. O'Keeffe, R.P. Brint, M.W.D. Mansfield, Chem. Phys. 217 (1997) 83.
[2] A. Maciejewski, M. Szymański, R.P. Steer, J. Chem. Phys. 90 (1986) 6314.
[3] M. Szymański, A. Maziejewski, R.P. Steer, Chem. Phys. 124 (1988) 143.
[4] A.A. Ruth, F.J. O'Keeffe, M.W.D. Mansfield, R.P. Brint, J. Phys. Chem. A 101 (1997) 7735.

[5] The vapour pressure of BPT near its melting point was assumed to be similar to that of 4-H-pyrane-4-thione (PT) close to its melting point. The temperature dependence of the vapour pressure of PT will be published in [21].

[5] A.A. Ruth, F.J. O'Keeffe, M.W.D. Mansfield, R.P. Brint, Chem. Phys. Lett. 264 (1997) 605.
[6] A. O'Keefe, D.A.G. Deacon, Rev. Sci. Instrum. 59 (1988) 2544.
[7] A. O'Keefe, J.J. Scherer, A.L. Cooksy, R. Sheeks, J. Heath, R.J. Saykally, Chem. Phys. Lett. 172 (1990) 214.
[8] D. Romanini, K.K. Lehmann, J. Chem. Phys. 99 (1993) 6287.
[9] T. Yu, M.C. Lin, J. Am. Chem. Soc. 115 (1993) 4371.
[10] T. Yu, M.C. Lin, J. Chem. Phys. 98 (1994) 9697.
[11] G. Meijer, M.G.H. Boogaarts, R.T. Jongma, D.H. Parker, A.M. Wodtke, Chem. Phys. Lett. 217 (1994) 112.
[12] R.T. Jongma, M.G.H. Boogaarts, G. Meijer, J. Mol. Spectr. 165 (1994) 303.
[13] P. Zalicki, Y. Ma, R.N. Zare, J.R. Dadamio, E.H. Wahl, T.G.Owano, C.H. Kruger, 47th Annual Gaseous Electronics Conference, Gaithersburg, Maryland, 1994.
[14] W. Demtröder, Laserspektroskopie, Springer–Verlag, Berlin, 1991, Chap. 5.2.
[15] J.T. Hodges, J.P. Looney, R.D. van Zee, J. Chem. Phys. 105 (1996) 10278.
[16] K.K. Lehmann, D. Romanini, J. Chem. Phys. 105 (1996) 10263.
[17] P. Zalicki, R.N. Zare, J. Chem. Phys. 102 (1995) 2708.
[18] J.J. Scherer, J.B. Paul, C.P. Collier, R.J. Saykally, J. Chem. Phys. 102 (1995) 5190, ibid. 103 (1995) 113, ibid. 103 (1995) 9187.
[19] H. Eisenberger, B. Nickel, J. Chem. Soc. Faraday Trans. 92 (1996) 733.
[20] T. Förster, Fluoreszenz Organischer Verbindungen, Vandenhoek & Ruprecht, Göttingen, 1951, p. 142, Eq. (26,6').
[21] T. Fernholz, A.A. Ruth, M.W.D. Mansfield, R.P. Brint, in preparation.
[22] J.B. Anderson, in: Molecular beams and low density gas dynamics, eds. P.P. Wegener, Marcel Dekker, New York, 1974, Vol. 4, p. 1.